THE ASTROPHYSICAL JOURNAL, 344:404–412, 1989 September 1

COLLIMATION OF STELLAR WINDS BY NONADIABATIC DE LAVAL NOZZLES

A. C. RAGA[1]
Astronomy Department, University of Washington
AND
J. CANTÓ
Instituto de Astronomía, Universidad Nacional Autónoma de México
Received 1988 October 7; accepted 1989 February 1

ABSTRACT

The interaction between an isotropic stellar wind and a stratified environment can lead to the formation of de Laval nozzles (in the adiabatic case) or to the formation of an elongated cavity surrounded by a dense, cold shell of shocked gas (in the limit of short cooling distances, i.e., in the highly nonadiabatic case). A preliminary exploration of the intermediate regime between the adiabatic and the highly nonadiabatic regimes yields very interesting results. We find that while for large cooling distances (i.e., cooling distances larger than ~ 5 times the environmental scale height) the flow resembles the adiabatic de Laval nozzle, for short cooling distances (i.e., cooling distances smaller than ~ 5 times the environmental scale height) the flow is considerably different from the adiabatic case, leading to the formation of very narrow, well collimated, cold jets. A preliminary comparison between observations of the HH 1/2 source and radio free-free spectra computed from our models gives very encouraging results.

Subject headings: hydrodynamics — stars: winds

I. INTRODUCTION

Regions of low mass star formation show the occurrence of well collimated, high-velocity outflows from protostars or young stellar objects (see, e.g., Mundt 1985). The regions of interaction between these outflows and their environment show a number of interesting observational characteristics. The Herbig-Haro objects, "cavities," and "jets" which are produced by these interactions have been the focus of quite extensive theoretical and observational studies in the recent past (see, e.g., the reviews of Mundt 1987 and Dyson 1987).

Some of the observed stellar outflows are very highly collimated, showing very thin jets (with unresolved or almost unresolved cross sections) extending outward from the central source of the outflow. Typical examples of this kind of object are the HH 34 (Reipurth *et al.* 1986; Raga and Mateo 1988; Bührke, Mundt, and Ray 1988) and the L1551 (Mundt, Brugel, and Bührke 1987; Campbell *et al.* 1988) jets. These objects show the necessary existence of mechanisms for producing very well collimated outflows during the process of stellar formation or early stellar evolution. The present paper consists of an exploration of a mechanism for the production of this kind of collimation.

A possible mechanism for the formation of collimated outflows has been explored in detail by Cantó (1980) and compared with observations by Cantó, Sarmiento, and Rodríguez (1986). A source with an isotropic wind is assumed to be located in a stratified environment, and the interaction between the wind and the environment leads to the formation of one or two (oppositely directed) elongated cavities. The apex of these cavities correspond to the starting points of well collimated jets (Cantó, Tenorio-Tagle, and Różycka 1988). A fundamental assumption of these models is that the flow is highly nonadiabatic, so that the stellar wind, which is shocked at the edges of the cavity, forms a thin, cold layer surrounding the cavity.

A similar scenario has been explored by Königl (1982), who suggested that for an *adiabatic* stellar outflow such a configuration would lead to the formation of one or two (oppositely directed) de Laval nozzles. This scenario had been previously proposed by Blandford and Rees (1974) for extragalactic outflows, and explored numerically and analytically by Norman *et al.* (1981) and Smith *et al.* (1983). As discussed by Dyson (1987), the Cantó and the Königl models correspond to the limits of high and low cooling efficiencies, respectively, for the problem of an isotropic wind source in a stratified environment.

In this paper we extend Königl's (1982) calculation of a de Laval nozzle flow to the nonadiabatic case. This allows us to explore a regime of moderate cooling which might be relevant for stellar outflows.

However, one has to be very cautious in interpreting the present models as an intermediate case between the Konigl and the Cantó models. Because of the way our approximate models have been constructed, while we can regain Konigl's (1982) results for adiabatic flows, we do not obtain a transition to the Cantó (1980) models for the highly nonadiabatic case. A study of whether or not a transition between the Cantó and Königl models actually occurs in real flows lies outside the scope of our simplified formulation.

II. THE NONADIABATIC DE LAVAL NOZZLE FLOW

a) Equations

Following Königl (1982), we assume that a source with an isotropic wind is located in a stratified environment. It is assumed that the stellar wind goes through a shock at a radius R_s, and is then channelled into two oppositely directed de Laval nozzles (see Fig. 1).

The calculation is carried out under the assumption that the motion of the gas is almost completely parallel to the axis of

[1] Now at the Canadian Institute for Theoretical Astrophysics.

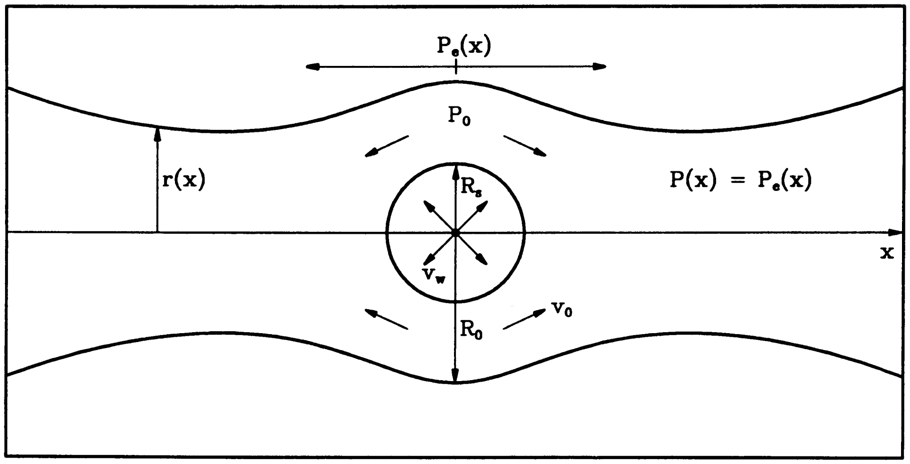

FIG. 1.—Schematic diagram showing the general configuration assumed for a de Laval nozzle flow. An isotropic wind source is located at the origin, and at a radius R_s the wind goes through a shock. The stratified environment [with a pressure stratification $P_e(x) = P_e(-x)$] collimates the wind into two oppositely directed de Laval nozzles (*see text*).

symmetry of the flow. This approximation is obviously not valid in the region close to the source, where the flow can have substantial velocities perpendicular to the axis of symmetry (as is intuitively obvious from Fig. 1).

On the other hand, the flow velocities close to the star (but outside the shock situated at a radius R_s; see Fig. 1) are subsonic, so that the main characteristics of the flow are determined to a large extent by pressure gradients (rather than by advection). Because of this, a precise knowledge of the velocity field is not essential for a determination of the general characteristics of the flow in this region. As Königl (1982) has done, we will assume that the radius R_s of the stellar wind shock is small (compared, e.g., to the scale height of the environment and to the cooling distance), and solve the problem under the assumption that velocities are almost parallel to the axis of symmetry throughout the flow.

For the environment, we assume (following Cantó 1980) a self-gravitating isothemal disk pressure stratification:

$$\frac{P_e(x)}{P_0} = \frac{4e^{x/H}}{(1 + e^{x/H})^2}, \tag{1}$$

where

$$H = \frac{P_0^{1/2}}{(8\pi G)^{1/2}\rho_{e,0}}, \tag{2}$$

G is the gravitational constant, and P_0 and $\rho_{e,0}$ are the environmental pressure and density, respectively, at $x = 0$ (see Fig. 1). This simple description of the environment as a self-gravitating slab is at best a very crude approximation to the stratification of a circumstellar disk, but it provides a convenient parametrization appropriate for the very simplified calculation we have carried out. The effects introduced by different environmental stratifications should be explored in the future, possibly in the context of more realistic de Laval nozzle models.

Under the assumption of flow motion almost parallel to the axis of symmetry (see above), the Euler equations take the simple form:

$$\rho v \pi r^2 = \text{const.} \tag{3}$$

(continuity equation),

$$\frac{d}{dx}\left(\frac{v^2}{2}\right) + \frac{1}{\rho}\frac{dP}{dx} = 0 \tag{4}$$

(equation of motion),

$$\frac{dh}{dx} = -\frac{L}{v}\,; \quad h = \frac{v^2}{2} + \frac{\gamma}{\gamma - 1}\frac{P}{\rho} \tag{5}$$

(energy equation), where x is the distance measured along the axis of symmetry, r is the cylindrical radius of the nozzle, ρ is the density, v the velocity (assumed to be parallel to the x-axis), P is the pressure, L the energy loss (per unit mass and time), and γ is the specific heat ratio of the gas (assumed to be constant throughout the flow). The gas is also assumed to be in pressure equilibrium with the environment:

$$P(x) = P_e(x)\,. \tag{6}$$

This approximation is valid provided that the ratio of the environmental scale height to the radius of the nozzle, H/r, is larger than the Mach number $M = v/c_s$ of the flow.

In order to carry out an integration of the flow equations, it is necessary to determine the value of the cooling function L (see eq. [5]). In order to determine the cooling of a non-adiabatic flow, it is in principle necessary to explicitly solve the ionization rate-of-change equations for all the ions in the gas (see, e.g., Kafatos 1973).

We have carried out a calculation of the cooling rate with the following simplified approach. It is possible to obtain an approximate estimate of the cooling rate by assuming that the gas continuously relaxes to coronal ionization equilibrium (i.e., collisional ionizations balanced by radiative and dielectronic recombinations). In this approximation, the ionization state of the gas is determined by the local temperature (and not by a number of complex ionization rate-of-change equations). If we additionally assume that all the collisional line excitation is occurring in the low density regime, the cooling rate is given by

$$L = \rho F(T)\,, \tag{7}$$

where ρ is the density and T the temperature of the gas, and $F(T)$ is a function which is determined by the coronal ionization equilibrium condition and all the cooling processes which occur in the gas. For this function, we have taken the approximate parametrized form:

$$F(T) = 2.21 \times 10^{29} \text{ (ergs s}^{-1}\text{ cm}^3\text{ g}^{-2})T^{-0.63} \times [1 - e^{-(T/10^5)^{1.63}}] \frac{r(T)}{1 + r(T)}, \quad (8)$$

where $r(T) = 0.244T^{1.2} \exp(-157900/T)$ is the ratio between the collisional ionization and radiative recombination rates for hydrogen, and temperatures are in Kelvins. Equation (8) represents an analytic approximation to the cooling function determined numerically by Raymond, Cox, and Smith (1976), for the $T = 10^4$–10^7 K temperature range.

We have assumed that hydrogen produces the most important contribution to the electron density (neglecting the contributions of other elements). In this approximation, the coronal equilibrium condition determines the temperature as a function of the pressure and density through

$$\frac{P}{\rho \Re} = T\left[\frac{1 + 2r(T)}{1 + r(T)}\right], \quad (9)$$

where $\Re$ is the gas constant, and the function $r(T)$ has been defined above (see eq. [8]). From equation (9) it is possible to obtain (numerically) the temperature as a function of the pressure and density of the gas: $T = T(P/\rho)$.

Writing distances in units of the scale height H of the environment ($x' = x/H$), the pressure in units of P_0 ($P' = P/P_0$), the velocity in units of the value $c_{s,0}$ of the speed of sound at $x = 0$ ($v' = v/c_{s,0}$), the density in units of $\rho_0 = \rho$ ($x = 0$) ($\rho' = \rho/\rho_0$), and defining $f(P'/\rho') = F(T)/F(T_0)$ (see eqs. [8] and [9]), equations (1)–(7) can be combined to obtain

$$\frac{d\rho'}{dx'} = \frac{\rho'}{\gamma}\left[\frac{1}{\kappa}\frac{\rho'^2 f(P'/\rho')}{v'P'} + \frac{\dot{P}'}{P'}\right], \quad (10)$$

$$\frac{dv'^2}{dx'} = -\frac{2}{\gamma}\frac{\dot{P}'}{\rho'}, \quad (11)$$

where

$$\frac{\dot{P}'}{P'} = \left(1 - \frac{2}{1 + e^{-x'}}\right) \quad (12)$$

is the logarithmic pressure gradient, and

$$\kappa = \frac{d_{\rm cool}}{H} = \frac{1}{H}\frac{P_0 c_{s,0}}{(\gamma - 1)\rho_0 L_0}, \quad (13)$$

is the ratio of the initial cooling distance $d_{\rm cool}$ (i.e., the cooling distance for $x = 0$) to the environmental scale height H (the subscript 0 indicates values for $x = 0$). The exact definition used for the cooling distance $d_{\rm cool}$ is given by equation (13).

b) *Boundary Conditions*

The problem now consists of integrating equations (10) and (11). For this integration, an appropriate choice of boundary conditions has to be carried out. Blandford and Rees (1974) and Königl (1982) have chosen the condition $v'(x' = 0) = 0$ (the other boundary condition is $\rho'(x' = 0) = 1$, a result of the fact that densities are given in units of ρ_0, see above). This choice of boundary conditions is based on the fact that the gas at radii slightly larger than R_s (see Fig. 1) has a high temperature and a low velocity, corresponding to the postshock conditions of the stellar wind shock. Even more, in the real, two-dimensional flow the velocity along the axis at $x' = 0$ is indeed 0, but the flow has a nonzero velocity along the equatorial plane (an effect which cannot be described in our simplified one-dimensional formulation).

However, the choice of $v'(x' = 0) = 0$ as a boundary condition has an important problem. The continuity equation (eq. [3]) implies that if the velocity goes to 0 while the density remains finite, the radius of the nozzle has to go to infinity. Because of this choice of boundary conditions, a divergence of the radius of the nozzle for $x' \to 0$ is present in the solutions of Blandford and Rees (1974) and Königl (1982). This divergence in principle is not a fundamental problem, because the simplifications introduced in the equations (i.e., the assumption of velocities almost parallel to the axis of symmetry) are not valid for $x' \to 0$, so that the low x' region of the obtained solution should anyway not be taken too seriously.

A somewhat more appropriate choice of boundary conditions can be obtained by noting that at low values of x' the velocity of the nozzle flow is not actually 0, but has a value which approximately corresponds to the velocity of the post–stellar wind shock (i.e., the shock situated at R_s; see Fig. 1). The conditions for a strong shock give us the value $v'(x' = 0) = 5^{-1/2}$, in units of the postshock sound speed $c_{s,0} = c_s(x' = 0)$.

This choice of boundary condition (which we will use for the following calculations) appears to be more appropriate than the boundary condition used by Blandford and Rees (1974) in that it does not produce an unphysical divergence in the nozzle radius for $x' \to 0$. On the other hand, both choices of boundary conditions are somewhat arbitrary because the simplified, one-dimensional equations actually cannot describe the nozzle flow close to the source (a region in which the velocities along and across the axis of symmetry have comparable magnitudes).

Because the cooling function (see eq. [7] and [8]) depends on the actual value T of the temperature (and not only on the dimensionless temperature T/T_0), in order to integrate the flow equations it is also necessary to specify the initial value of the temperature $T_0 = T(x' = 0)$. The necessity of specifying the initial temperature as a boundary condition disappears if one considers power-law cooling functions (which are scale-free). This appears to be a clear advantage for a preliminary exploration of the problem, such as we are carrying out in this study. Unfortunately, it is not possible to define a unique power-law index for the temperature range $T = 10^4$–10^7 K relevant to stellar outflows (see, e.g., Cox and Daltabuit 1971). One would have to obtain solutions for a range of power-law indices, in this way introducing again an extra free parameter.

Even though in our simplified equations (eq. [10] and [11]) the region of radii comparable to R_s is not properly described, it is still possible to relate (in an approximate way) the parameters of the nozzle flow to the stellar wind parameters.

The approximate equilibrium between the ram pressure of the stellar wind and the environmental pressure ($P_0 = \rho_w v_w^2$) determines the positon of the stellar wind shock:

$$R_s = \left(\frac{\dot{M} v_w}{4\pi P_0}\right)^{1/2}, \quad (14)$$

where $\dot{M}$ is the mass-loss rate, and v_w is the stellar wind velocity.

Another important relation can be obtained by noting that half of the mass going through the stellar wind shock has to go out through each nozzle (see Fig. 1). Under the assumption that R_s is much smaller than the scale of variation of the nozzle radius (see above), this leads to the simple relation:

$$\frac{\dot{M}}{2} = \pi R_0^2 \rho_0 v_0 , \qquad (15)$$

where R_0 is the radius of the nozzle at $x = 0$ (see Fig. 1). In the derivation of equation (15) we have assumed that the material in the nozzle flow comes exclusively from the stellar wind. Effects like evaporation from the cavity walls under certain conditions might produce a substantial contribution to the material in the nozzle flow.

Considering that the mass loss rate can also be written as $\dot{M} = 4\pi R_S^2 \rho_0 v_0$, from equation (15) we see that $R_0 = 2^{1/2} R_s$. This relation, together with equation (14) allows us to obtain predictions of nozzle flows for different stellar wind parameters from our approximate calculations.

c) *Numerical Integration*

We have integrated equations (10) and (11) numerically with a fourth-order, adjustable step size Runge-Kutta method. The boundary conditions described in § II*b* have been used. An exploration of the solutions for different initial temperatures T_0 and values of the ratio $\kappa = d_{\rm cool}/H$ gives very interesting results.

We have carried out numerical integrations for initial temperatures $T_0 = 10^5$ K (see Fig. 2), 5×10^5 K (Fig. 3) and 10^7 K (Fig. 4), and for a few values of κ ranging from $\kappa = 1$ to ∞ ($\kappa = \infty$ corresponds to the adiabatic case).

The numerical integration of the equations for a nonadiabatic de Laval nozzle flow has given very interesting results. The introduction of an energy loss term produces nozzles with higher collimation than in the adiabatic case. For the higher κ values which we have computed (Figs. 2–4), the solutions always look qualitatively similar to the adiabatic solution, but the nonadiabatic nozzles always show a higher degree of collimation, higher density, lower velocity and temperature, and a higher Mach number than the adiabatic nozzle.

For low κ values (Figs. 2–4) qualitatively very different results are obtained. For example, the nozzle radius r as a function of the distance x from the star initially follows the adiabatic solution, but then starts to decrease more and more

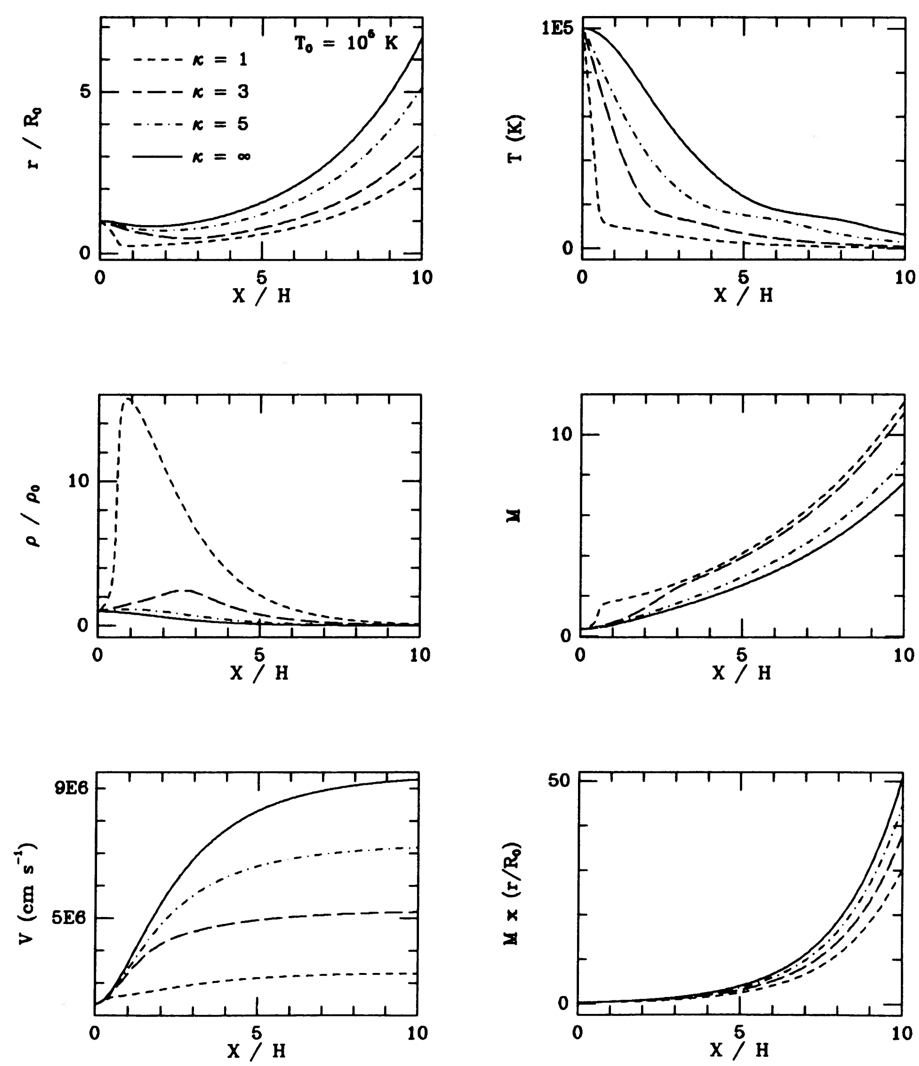

FIG. 2.—Stratification obtained for de Laval nozzles with different values of $\kappa = d_{\rm cool}/H$ and initial temperature $T_0 = 10^5$ K. The left-hand column shows the radius (*top*), density (*center*), and velocity (*bottom*), and the right-hand column shows the temperature, Mach number and the product $M \times (r/R_0)$ as a function of the dimensionless distance x/H (*see text*).

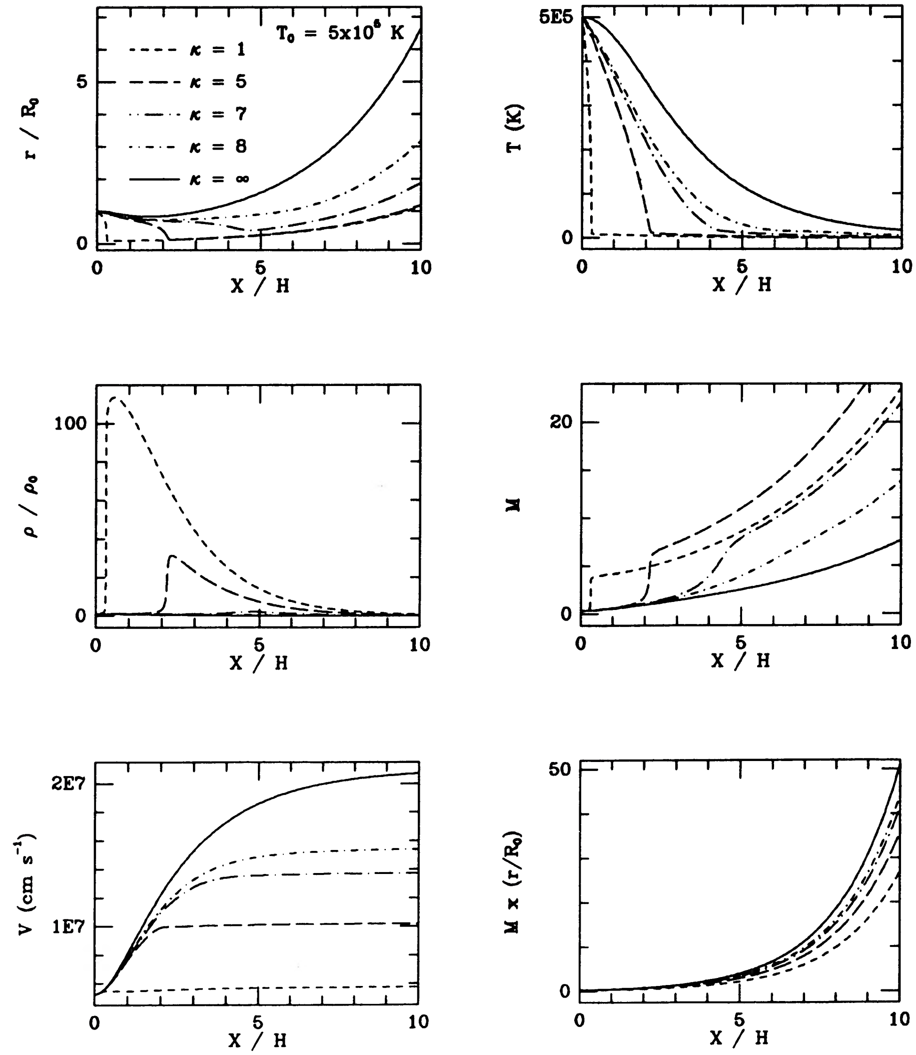

FIG. 3.—The same as Fig. 2, but for nozzles with an initial temperature $T_0 = 5 \times 10^5$ K.

rapidly. This "collapse" of the nozzle radius eventually stops when the gas recombines (causing the cooling rate to drastically decrease), and for larger values of x a very narrow, slowly opening "jet" is obtained.

This effect is most pronounced in our $T_0 = 10^7$ K calculation (see Fig. 4) where we observe the formation of very thin jets for $\kappa = 1$–10. The region in which the nozzle collapses to form a thin jet shows a sharp increase in the density and the Mach number of the flow. At larger values of x (i.e., in the "jet" region of the flow) the density starts to decrease, the velocity of the flow is approximately constant, and the Mach number continues to increase (because of the temperature decrease brought about by the adiabatic cooling of the gas).

In Figures 2–4 we have also plotted the product $M \times r/R_0$. As we have discussed above, the approximation of setting the pressure $P(x)$ of the flow equal to the local environmental pressure $P_e(x)$ (see eq. [6]) is valid only if the environmental scale height H is larger than $r \times M$ where r is the radius and M the local Mach number of the nozzle flow. For $x = 0$, $M \times r/R_0 = 5^{-1/2}$, so that the criterion for $P(x) \approx P_e(x)$ is satisfied for initial nozzle radii $R_0 \leq 5^{1/2} \times H$. On the other hand (as is clear from Figs. 2–4) even if $H/R_0 \geq M \times r/R_0$ for low values of x (i.e., for $r \approx R_0$), the value of the right-hand term of this inequality grows with increasing x, so that for large enough values of x this inequality will no longer be satisfied.

In other words, for large values of x, the approximation of setting the flow pressure equal to the local environmental pressure (on which our calculations are based) eventually breaks down. From this point onward, the flow will be overpressured with respect to the local environment. It is not possible to study this region of the flow with the set of simplifying assumptions which we have used in the present calculations. We leave this description of an "overpressured jet" flow for a future paper.

We also note the following interesting fact. For $\kappa = d_{\rm cool}/H \to 0$, our solutions do not correspond anymore to the real physical situation found in a stellar outflow. Our calculations are based on the assumption that the flow is almost parallel to the symmetry axis of the flow, a condition which is only satisfied if the cooling distance $d_{\rm cool}$ is much larger than the radius R_S of the stellar wind shock (see Fig. 1). The $\kappa = d_{\rm cool}/H \to 0$ regime of this flow has previously been analyzed in detail by Cantó (1980) with a different set of simplifying assumptions.

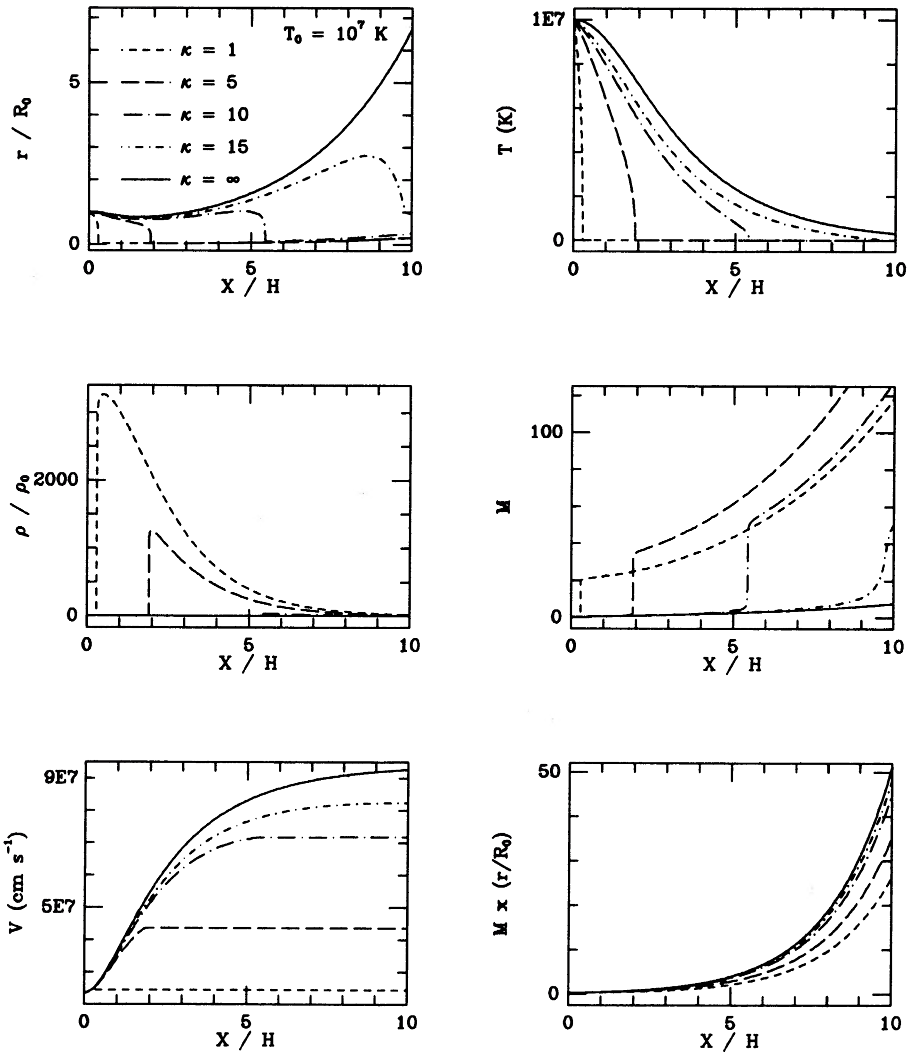

FIG. 4.—The same as Fig. 2, but for nozzles with an initial temperature $T_0 = 10^7$ K.

The condition of flow almost parallel to the axis of symmetry also is not correct for another region of the flow. As we have discussed above, for low κ values the nozzle collapses to form a narrow, jet-like flow (see also Figs. 2–4). In the region where the narrow jet is formed, substantially large radial flow velocities might be produced, leading to the formation of rarefaction waves and shock waves. This region of the flow is obviously not properly described by our simple one-dimensional equations, so that considerable deviations from our simplified solutions might be expected. We expect that the general result implying the formation of a narrow jet by the collapse of a de Laval nozzle (due to a strong radiative cooling) should still be correct, at least in a qualitative way.

It is interesting to estimate the rate at which kinetic energy is deposited by the de Laval nozzle at $x \to \infty$ as a function of κ. In Figure 5, we have plotted this rate as a fraction of the rate of kinetic energy input from the stellar wind (this quantity corresponds to a kinetic energy "efficiency") for the three different initial temperatures which we have considered. We have stopped the curves at $\kappa = 1$ to stress the fact that our present simplified model breaks down at low κ values. The highest efficiency is obtained in the adiabatic case ($\kappa \to \infty$), for which the kinetic energy efficiency has a value of $\frac{1}{2}$ (i.e., one-half of the kinetic energy of the wind is deposited at the end of each of the two de Laval nozzles). For the low κ regime, a considerably smaller (but finite) efficiency is obtained.

This result indicates that highly nonadiabatic de Laval nozzles (with low κ values) are not as efficient as adiabatic nozzles in transferring the energy of an isotropic wind into a collimated outflow. On the other hand, low κ nozzles are able (as we have seen above) to produce a much higher degree of collimation than adiabatic nozzles.

III. THE FREE-FREE CONTINUOUS SPECTRUM AND THE HH 1/2 SOURCE

The sources of bipolar outflows generally are very highly obscured, so that they are many times not visible at optical wavelengths (except for a few noteworthy cases, e.g., the sources of HH 32 and HH 57). For example, the source of the HH 1/2 system (which is one of the brightest and better understood systems of Herbig-Haro objects) is not visible at optical wavelengths (see, e.g., Strom *et al.* 1985), and has been discovered at radio wavelengths by Pravdo *et al.* (1985). A detailed discussion of infrared observations of this object has

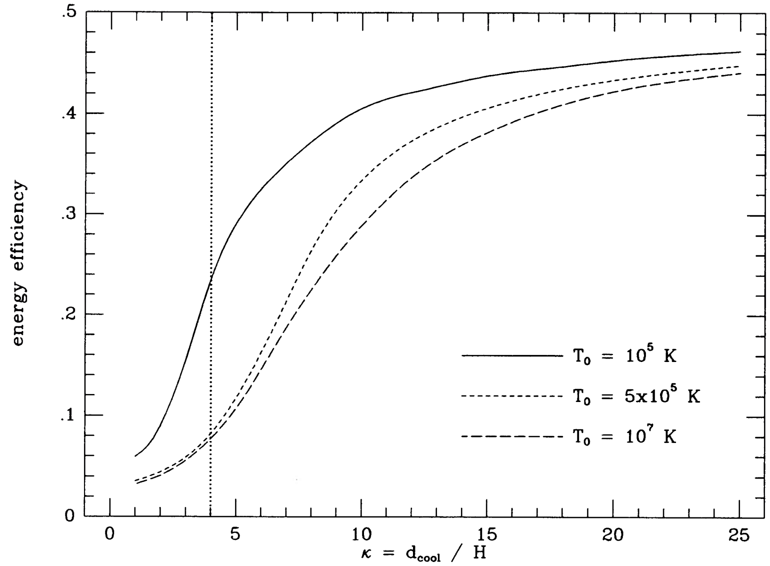

FIG. 5.—Efficiency of a de Laval nozzle for depositing kinetic energy from the stellar wind into a collimated outflow as a function of κ (*see text*). For $\kappa \to \infty$, the energy efficiency reaches an asymptotic value of $\frac{1}{2}$, indicating that one-half of the total kinetic energy produced by the wind (per unit time) ends up being deposited in each of the two de Laval nozzles which are produced in this scenario. Curves for nozzles with initial temperatures $T_0 = 10^5$, 5×10^5, and 10^7 K are shown.

been carried out by Tapia *et al.* (1987). Pravdo *et al.* (1985) have observed a spectrum with a spectral index of 0.4 ± 0.2 for the source of the HH 1/2 system (recent observations made by Rodríguez *et al.* 1988 show a spectral index of 0.3 ± 0.1). Because of this remarkable observation, it is interesting to try to obtain approximate predictions of the radio spectrum from our nonadiabatic de Laval nozzle models.

We have computed S_ν from our models by integrating numerically the radiative transfer equation:

$$S_\nu = \frac{2k\nu^2}{c^2} \iint T(x)[1 - e^{-\tau_\nu(x,r')}]dr'\,dx\,, \qquad (16)$$

where

$$\tau_\nu(x, r') = 7.57 \times 10^{46}[\rho(x)y_{\mathrm{H}^+}(x)]^2[T(x)]^{-1.35}\nu^{-2.1} \times \frac{r'}{r(x)}\{[r(x)]^2 - r'^2\}^{1/2}\ \mathrm{cm}^{-1} \qquad (17)$$

and k is Boltzmann's constant, c is the speed of light, ν is the frequency, and $T(x)$, $\rho(x)$, $r(x)$ and $y_{\mathrm{H}^+}(x)$ are the temperature, density, radius, and hydrogen ionization fraction obtained from our nonadiabatic de Laval nozzle models.

In Figure 6 we show the resulting spectrum, giving the values of S_ν/S_{ν_0} as a function of the dimensionless frequency ν/ν_0 for nozzles with different values of κ and initial temperatures $T_0 = 10^5$ K, 5×10^5 K and 10^7 K. The frequency ν_0 is defined as the frequency for which a column of length R_0 of gas with a density ρ_0 and temperature T_0 (the values for the $x = 0$ region of the nozzle; see Fig. 1) has an optical depth of 1:

$$\nu_0 = [7.57 \times 10^{46}(\rho_0\, y_{\mathrm{H}^+,0})^2 T_0^{-1.35} R_0]^{0.476}\,. \qquad (18)$$

From Figure 6, we see that in all cases there is a transition from the optically thick (ν^2) regime for $\nu \ll \nu_0$ to the optically thin ($\nu^{-0.1}$) regime for $\nu \gg \nu_0$. The extent of the range of frequencies over which this transition occurs depends on the initial temperature and cooling distance of the nozzle flow (low κ nozzles show a more extended transition than high κ nozzles).

For example, for a nozzle with central temperature $T_0 = 5 \times 10^6$ K, number density $n_0 \approx \rho_0/m_{\mathrm{H}} = 2 \times 10^5\ \mathrm{cm}^{-3}$ and radius $R_0 = 10^{15}$ cm, we obtain a value $\nu_0 \approx 6.4 \times 10^8\ \mathrm{s}^{-1}$, corresponding to a wavelength $\lambda_0 \approx 50$ cm. For these parameters (which might or might not be appropriate for the case of the HH 1/2 source) the observations of Pravdo *et al.* (1985) (carried out at wavelengths of 2, 6, and 20 cm) would correspond to frequencies of $\nu \sim (2\text{–}20) \times \nu_0$. From Figure 6, we see that low κ de Laval nozzles (e.g., the $\kappa = 1$ or $\kappa = 5$ nozzles with $T_0 \geq 5 \times 10^5$ K) produce a spectrum with a low (but positive) spectral index for this frequency range, in qualitative agreement with the results of Pravdo *et al.* (1985).

The parameters chosen above are consistent with other observational properties of the HH 1/2 system in the following sense. We find that a $T_0 = 5 \times 10^6$ K, $\kappa = 5$ nozzle produces a "cold jet" with a terminal velocity of $\sim 300\ \mathrm{km\ s}^{-1}$. This velocity is of the same order of magnitude as the velocities deduced from the proper motions of the condensations of HH 1 and 2 (the largest of which approximately correspond to $350\ \mathrm{km\ s}^{-1}$; see Herbig and Jones 1981).

Also, we can use the relations between stellar wind parameters and nozzle flow parameters sketched in § II*b* to obtain the characteristics of the stellar wind. From the above parameters we obtain a mass loss rate $\dot{M} \sim 4 \times 10^{-7}\ M_\odot\ \mathrm{yr}^{-1}$ and a wind velocity $v_w \sim 500\ \mathrm{km\ s}^{-1}$. This gives a value for the kinetic luminosity of the wind: $L_w = \dot{M}v_w^2/2 \sim 8\ L_\odot$.

This result allows us to estimate the kinetic luminosity of the collimated outflow. Using the result that a $T_0 = 5 \times 10^6$ K, $\kappa = 5$ nozzle has an "energy efficiency" of ~ 0.1 (see § II*c* and Fig. 5), we obtain a kinetic luminosity for the outflow: $L_{\mathrm{out}} \sim 0.8\ L_\odot$. This value of L_{out} agrees qualitatively well with the values estimated by Brugel, Böhm, and Mannery, (1981) for the luminosities of HH 1 and 2.

From the above discussion, we conclude that the observations of the source of the HH 1/2 system can indeed be explained in terms of a nonadiabatic de Laval nozzle. A nozzle with $\kappa = d_{\mathrm{cool}}/H \sim 5$ could produce a free-free radio spectrum with a spectral index consistent with the observations of

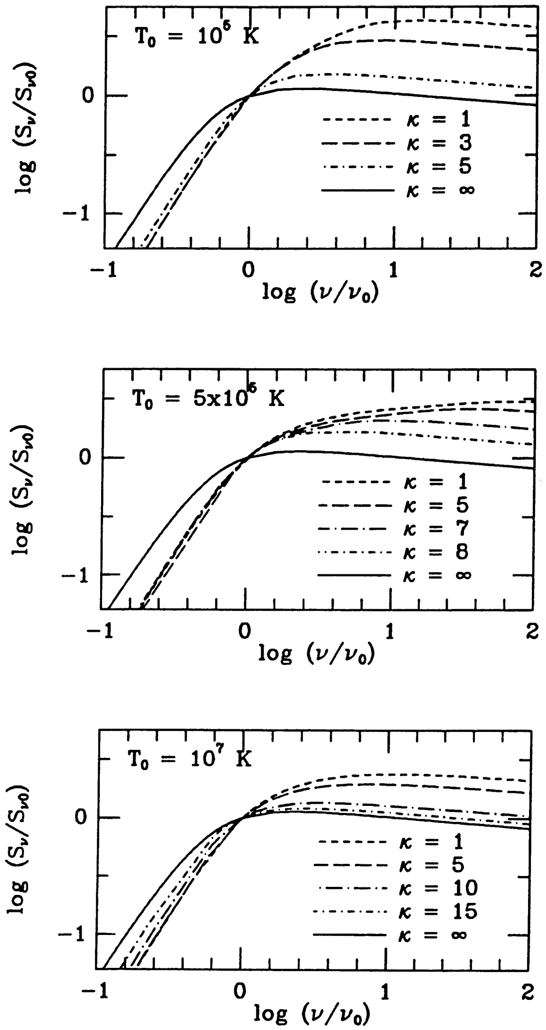

FIG. 6.—Radio free-free continuous spectrum predicted from de Laval nozzle flows with different κ values. The definition of the value of the frequency ν_0 (which is used to adimensionalize the frequencies and the fluxes) is given in the text. For decreasing values of κ, more extended transition regions between the optically thick (ν^2) and the optically thin ($\nu^{-0.1}$) regimes are obtained. Results for nozzles with initial temperatures $T_0 = 10^5$ (*top*), 5×10^5 (*center*), and 10^7 K (*bottom*) are shown.

Pravdo *et al.* (1985), and at the same time be consistent with the velocities and proper motions observed for the Herbig-Haro objects 1 and 2.

Let us finish the discussion of the HH 1/2 source with the following point. As we have described in §§ II*a* and II*c* our simplified nonadiabatic de Laval nozzle calculations are only applicable when the condition $H/r > v/c_s$ is met. For the parameters which we have suggested for the HH 1/2 source, from equations (8) and (13) we obtain a value $d_{\rm cool} = 8.2 \times 10^{15}$ cm for the initial cooling distance (implying a value of $H = d_{\rm cool}/\kappa = 1.64 \times 10^{15}$ cm for the environmental scale height). With these results we obtain $H/R_0 \approx 1.6$, which is considerably larger than the initial Mach number $v_0/c_{s,0} = 5^{-1/2}$ (see § II*b*), indicating that at least for low x values the flow indeed has a pressure similar to the environmental pressure (as has been assumed in our calculations). From this we conclude that our calculation of a pressure-matched de Laval nozzle is at least approximately applicable for the flow parameters discussed above.

We should note that the problem of prediction of radio free-free spectra from collimated outflows has been studied in considerable detail by Reynolds (1986). It is very difficult, however, to compare our results with those of Reynolds (1986), since we have carried out predictions from an actual flow model (in which hydrodynamic and ionization effects are calculated in an approximate, but self-consistent way) while Reynolds has carried out predictions from purely kinematic models (in which the flow has an assumed stratification, which is not actually calculated by solving the hydrodynamic equations).

IV. CONCLUSIONS

We have carried out simplified calculations of a nonadiabatic de Laval nozzle flow. These models describe the collimation of an isotropic stellar wind by a stratified environment, in a regime intermediate between the highly nonadiabatic regime assumed in the model of Cantó (1980) and the adiabatic regime assumed in the model of Königl (1982).

The solutions to the nonadiabatic de Laval nozzle flow depend strongly on the initial temperature T_0 of the flow and on the value of the dimensionless parameter κ, defined as the ratio between the initial cooling distance of the flow and the scale height of the environment (which is assumed to have a self-gravitating, isothermal slab stratification).

From numerical integrations of the simplified flow equations, we have determined that while for high κ values the solution resembles the adiabatic de Laval nozzle, for low values of κ surprising differences appear. In the low κ (i.e., high cooling) regime the radius of the nozzle rapidly decreases with increasing distance from the source, leading to the formation of a very well collimated, cold ($T \sim 10{,}000$ K) jet.

We have carried out a qualitative comparison between the radio free-free spectrum predicted from our models and observations of the source of the HH 1/2 system (by Pravdo *et al.* 1985). We find that a nozzle with $\kappa \sim 5$ can produce a spectrum with approximately the correct spectral index, and at the same time explain the velocities and luminosities observed for the Herbig-Haro objects HH 1 and 2. Even though this result does not conclusively prove that the HH 1/2 outflow is indeed produced by a nonadiabatic nozzle, it shows that these new models offer an attractive possible explanation for the production of bipolar outflows from young stars.

We would like to thank Karl-Heinz Böhm, Luis Rodríguez, and Alberto López for their helpful comments about the research described in this paper. We would also like to thank Arieh Königl (the referee) for suggesting improvements and pointing out mistakes in the original manuscript. A. C. R.'s work has been supported by the NSF grant AST 87-17867.

REFERENCES

Blandford, R. D., and Rees, M. J. 1974, *M.N.R.A.S.*, **169**, 395.
Brugel, E. W., Böhm, K. H., and Mannery, E. 1981, *Ap. J. Suppl.*, **47**, 117.
Bührke, T., Mundt, R., and Ray, T. 1988, *Astr. Ap.*, **200**, 99.
Campbell, B., Persson, S. E., Strom, S. E., and Grasdalen, G. L. 1988, preprint.
Cantó, J. 1980, *Astr. Ap.*, **86**, 327.
Cantó, J., Sarmiento, A., and Rodríguez, L. F. 1986, *Rev. Mexicana Astr. Ap.*, **13**, 107.
Cantó, J., Tenorio-Tagle, G., and Różycka, M. 1988, *Astr. Ap.*, **192**, 287.

Cox, D. P., and Daltabuit, E. 1971, *Ap. J.*, **167**, 113.
Dyson, J. E. 1987, *IAU Symposium 122, Circumstellar Matter*, ed. I. Appenzeller and C. Jordan (Dordrecht: Reidel), p. 159.
Herbig, G. H., and Jones, B. F. 1981, *A.J.*, **86**, 1232.
Kafatos, M. 1973, *Ap. J.*, **182**, 433.
Königl, A. 1982, *Ap. J.*, **261**, 115.
Mundt, R. 1987, *IAU Symposium 122, Circumstellar Matter*, ed. I. Appenzeller and C. Jordan (Dordrecht: Reidel), p. 147.
Mundt, R., Brugel, E. W., and Bührke, T. 1987, *Ap. J.* **319**, 275.
Norman, M. L., Smarr, L., Wilson, J. R., and Smith, M. D. 1981, *Ap. J.*, **247**, 52.
Pravdo, S. H., Rodríguez, L. F., Curiel, S., Cantó, J., Torrelles, J. M., Becker, R. M., and Sellgren, K. 1985, *Ap. J. (Letters)*, **293**, L35.
Raga, A., and Mateo, M. 1988, *A.J.*, **95**, 543.
Raymond, J. C., Cox, D. P., and Smith, B. W. 1976, *Ap. J.*, **204**, 290.
Reipurth, B., Bally, J., Graham, J. A., Lane, A., and Zealy, W. J. 1986, *Astr. Ap.*, **164**, 51.
Reynolds, S. P. 1986, *Ap. J.*, **304**, 713.
Rodríguez, L. F., Ho, P. T., Torrelles, J. M., Curiel, S., and Cantó, J. 1989, *Ap. J.*, submitted.
Smith, M. D., Smarr, L., Norman, M. L., and Wilson, J. R. 1983, *Ap. J.*, **264**, 432.
Strom, S. E., Strom, K. M., Grasdalen, G. L., Sellgren, K., Wolff, S., Morgan, J., Stocke, J., and Mundt, R. 1985, *A.J.*, **90**, 2281.
Tapia, M., Roth, M., Carrasco, L., and Ruíz, M. T. 1987, *M.N.R.A.S.*, **224**, 587.

J. CANTÓ: Instituto de Astronomía, Observatorio Astronómico Nacional de México, Apdo. Postal 70–264, Ciudad Universitaria, 04510 México, D.F., México

A. C. RAGA: McLennan Physical Laboratories, Canadian Institute for Theoretical Astrophysics, 60 St. George Street, Toronto, ON, Canada, M5S 1A1